AIAA JOURNAL
Vol. 36, No. 11, November 1998

Numerical Analysis of Shock Wave Reflection Transition in Steady Flows

M. S. Ivanov,* G. N. Markelov,† A. N. Kudryavtsev,‡ and S. F. Gimelshein†
Institute of Theoretical and Applied Mechanics, 630090 Novosibirsk, Russia

Different aspects of the transition between regular and Mach reflections of strong shock waves in steady flows are numerically studied. Two approaches—kinetic (the direct simulation Monte Carlo method) and continuum (Euler equations)—are used to investigate the hysteresis phenomenon in the flow about two symmetrical wedges in two- and three-dimensional statements. The dependence of the final shock wave configuration on initial conditions, the transition from regular to Mach reflection by means of flow perturbations, and three-dimensional effects are examined. The three-dimensionality of the flow is shown to increase the angles of transition from regular to Mach reflection and back and to decrease the Mach stem height.

Introduction

THE hypothesis that a hysteresis phenomenon may exist in the transition between regular reflections (RR) and Mach reflections (MR) of strong shock waves in steady flows was first put forward by Hornung et al.[1] They assumed that, when the angle of incidence α changes smoothly, the transition from RR to MR and the reverse transition occur at different α values. An attempt to assess this hypothesis was performed experimentally by Hornung and Robinson[2] and gave a negative result: No hysteresis was observed. They concluded that a possible reason might be the disturbances present in wind-tunnel flow.[2] Recently, though, the hysteresis was obtained experimentally by Chpoun et al.[3,4] and numerically by Ivanov et al.[5] using the direct simulation Monte Carlo (DSMC) method. In later papers by Ivanov et al.[6–9] the hysteresis phenomenon was examined carefully using two numerical approaches: kinetic and continuum. These numerical studies proved the existence of the hysteresis in accordance with the prediction of Hornung et al.[1] As for the experimental results of Chpoun et al.,[3,4] some details of this work, such as the angle of transition from RR to MR, α_{tr}, do not correspond to what comes from the hypothesis of Hornung et al.[1] (α_{tr} was 37.2 deg instead of $\alpha_D = 39.3$ deg for $M = 4.96$). This was probably caused by three-dimensional effects, which were fairly significant in these experiments, where a wedge model with a small spanwise size was used. The contradiction motivated conducting new experiments[10] where different aspect ratios, i.e., ratios of spanwise to streamwise size, from 0.66 up to 3.75, were used. The existence of hysteresis was confirmed there, but the total agreement of experimental and numerical data was not obtained.

The difficulties of experimental studies of the hysteresis phenomenon are caused by acoustic and other perturbations inherent in any aerodynamic wind tunnel and also the problem of obtaining results with no influence of three-dimensionality. These difficulties may be easily avoided if a numerical simulation is performed. The numerical approach gives an opportunity of not only assessing the impact of different perturbations and three-dimensionality but also elaborating a strategy for future experimental work. This paper is aimed at continuing the numerical study of various aspects of the problem. New results are presented on the influence of initial conditions on the final shock configuration, the transition between RR and MR caused by flow perturbations, and the role of three-dimensional effects.

Presented as Paper 97-2511 at the AIAA 32nd Thermophysics Conference, Atlanta, GA, June 23–25, 1997; received Nov. 26, 1997; revision received July 10, 1998; accepted for publication July 26, 1998.

*Head, Computational Aerodynamics Laboratory. E-mail: ivanov@itam.nsc.ru. Senior Member AIAA.
†Research Scientist, Computational Aerodynamics Laboratory.
‡Senior Research Scientist, Computational Aerodynamics Laboratory.

Some background information about shock reflections is given in the next section. Then, the flow conditions and details of numerical approaches are described. Afterward, the results of two- and three-dimensional computations are presented.

Background: RR and MR

For a wedge-generated oblique shock wave being reflected on the symmetry plane in a steady flow, two reflection types are possible: regular and irregular (e.g., see Ref. 2). In the first case (Fig. 1a), a reflected shock wave (RS) is formed at the intersection point of the incident shock (IS) and the symmetry plane. The flow that passes through the RS returns to its original direction parallel to the symmetry plane. For irregular reflection (MR; Fig. 1b), the point T where the incident and reflected shocks intersect is located at some distance from the symmetry plane and connected with it by the third shock wave, Mach stem (MS). Besides three shock waves, a slip surface (SS) also comes from the triple point T and divides the streams that passed through the MS and the two shocks, IS and RS. The existence of MR in steady flow is connected with the presence of the length scale (the wedge length w) that controls the MS height H_{st}. The trailing edge of a wedge generates an expansion fan that refracts on the RS and then interacts with the SS. Because of this interaction, the slip surface becomes curved and forms "a virtual nozzle."[2] In this nozzle the flow, turned to subsonic after passing through the MS, accelerates up to a supersonic velocity. Finally, the MS height is defined by the relation between the inlet and throat cross-sectional areas of the nozzle.

The transition from one reflection type to the other at a fixed freestream Mach number occurs at a certain angle α_{tr} between the incident shock and the symmetry plane. The analysis of two-shock and three-shock configurations[11] allowed the derivation of two principal criteria for strong shock waves ($M > 2.2$): the von Neumann criterion α_N and the detachment criterion α_D at which the transition from regular to MR may occur. Regular reflection is impossible for $\alpha > \alpha_D$, and MR is impossible for $\alpha < \alpha_N$. In the range $\alpha_N < \alpha < \alpha_D$ (dual solution domain) both reflection types are theoretically possible. The value of $(\alpha_D - \alpha_N)$ increases considerably when increasing M. For example, it reaches 8.5 deg for $M = 5$ (Fig. 2).

The theoretical possibility of the existence of two different shock configurations for $\alpha_N < \alpha < \alpha_D$ results in a question: Which criterion is correct for the transition between these configurations? The numerical investigations[5–8,12,13] manifested the hysteresis phenomenon, i.e., the reflection-type dependence on the direction of the incidence angle variation, at α changing through the range $\alpha_N < \alpha < \alpha_D$, both from below and from above. The transition from RR to MR in most papers occurs in accordance with the detachment criterion, and the reverse transition takes place near α_N.

The change of the base shape (angle ϕ variation within the range $0 \le \phi \le 90$ deg; Fig. 1a) does not impact significantly the transition

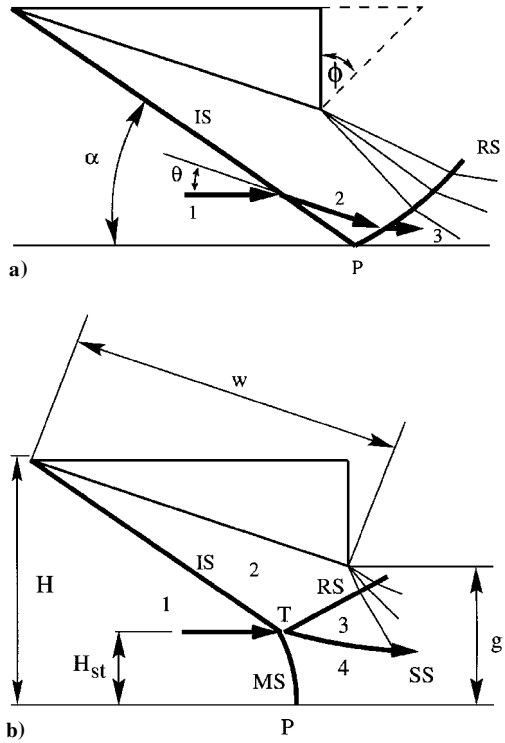

Fig. 1 a) Regular and b) Mach shock wave configurations.

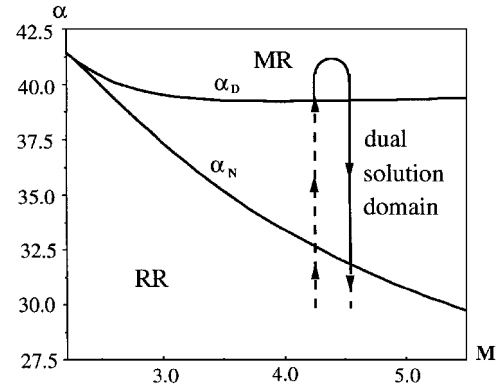

Fig. 2 Transition criteria and attendant hysteresis effect.

angles, the MS height, and other important characteristics of the flow.[14] The comparison of the numerical transition angles for two-wedge[5–8] ($\phi = 0$ deg) and channel[15] ($\phi = 90$ deg) geometries shows that they are independent of ϕ. Though the analytical models[16,17] give contradictory predictions concerning the dependence of the MS size on ϕ, there is numerical[18] and experimental[19] evidence that its size does not depend on the base angle either.

The steady MR can also be observed in supersonic jets. One example is the reflection of a shock generated at the edge of the nozzle operating under highly overexpanded flow conditions.[20–22] Therefore, the hysteresis phenomenon can be expected to be observed here. Indeed, the computations of plane jet flows performed by Ivanov et al.[9] for the jet Mach number $M = 4.96$ show the existence of both regular and MR at the same shock wave angle $\alpha = 36$ deg within the dual solution domain. Obviously, many different aspects of the phenomenon require further examination.

In two-dimensional computations, supersonic flows around two symmetrical wedges with $\phi = 0$ and 90 deg (a channel with a ramp) are considered to examine the transition between RR and MR. Because the problem is symmetric, only the upper half of the domain was considered in computations. Essential parameters for a two-dimensional case, besides the freestream Mach number M, are the incident shock wave angle α and the ratio g/w (see Fig. 1b). In all computations $M = 4.96$ and $g/w = 0.34$. This corresponds to the experimental conditions.[2–4,10] Perfect gas with a specific heat ratio $\gamma = 1.4$ was used.

The flow around two symmetrical wedges with $\phi = 0$ and a finite spanwise size z was investigated in three-dimensional computations. An additional parameter here is the aspect ratio z/w. To examine three-dimensional effects, the computations were performed for different aspect ratios. In addition to the horizontal symmetry plane between the wedges, there was the vertical symmetry plane, and the computations were performed in a quarter of the domain. The spanwise boundary was chosen far enough from the side wall to specify on it the inflow parameters corresponding to the freestream conditions.

Numerical Techniques

In spite of apparent simplicity, the numerical simulation of the transition between RR and MR and the investigation of the hysteresis phenomenon in a steady flow is a severe problem for various computational fluid dynamics methods. First, the dual-solution domain is large enough only for high Mach numbers. The flow therefore includes strong shock waves and a very low-density region behind the wedge that appears to be a problem for many solvers. Second, the flow under consideration has a few subtle details such as unsteady phenomena that are connected with physical instability of the slip surface and the wake flow. Finally, the nature of the flow investigated, which demonstrates the existence of two steady solutions and the hysteresis, requires an accurate numerical technique to be used.

In the present work, two numerical approaches have been used: the kinetic one, based on the solution of the Boltzmann equation by the DSMC method, and the continuum one that uses the solution of Euler equations. The application of two different approaches turns out to be beneficial for obtaining credible data on shock wave reflections.

Kinetic Approach

Being applied to the problem under consideration, the DSMC method has several important advantages. This approach takes into account viscosity, and the finite thickness of shock waves is physically grounded. The development of fast computers and parallel algorithms allows one to use the DSMC method for computing flows at very small Knudsen numbers, $Kn \leq 0.001$, and this method has become a powerful tool for modeling near-continuum flows. The computations for these Knudsen numbers enable one to obtain the shock wave configurations that are close to the solution of Euler equations. This is connected with the fact that the Knudsen number Kn affects only the thickness of shock waves. Outside the shock waves, the number of collisions is large enough to maintain a local equilibrium inherent in continuum flows. The shock wave configurations therefore do not depend on the Knudsen number.

The majorant frequency schemes[23] of the DSMC method were used in computations. A combined usage of cell and free cell schemes allowed us to achieve high spatial resolution in the entire flowfield, including the regions of large gradients. A rectangular grid with a variable cell size was used. The cell size depends on the local mean free path. The variable hard sphere model was used for the molecular potential. The energy exchange between the translational and rotational modes follows the Larsen–Borgnakke model[24] with the rotational relaxation number $Z_r = 5$.

The freestream conditions with Maxwellian distribution functions were assigned at the upstream and upper boundaries of the domain. The downstream boundary was chosen in such a way that the flow there was supersonic, and the vacuum conditions were specified for it, i.e., no particles entering the computational domain. To avoid the boundary-layer formation, specular reflection was used on the wedge surface.

To reduce the influence of statistical dependence between the model particles and to provide an adequate spatial resolution, the number of molecules in two-dimensional computations was varied within the range of 4×10^5–5×10^6 depending on the Knudsen number, and the number of cells was 10^5–10^6. In three-dimensional

computations the numbers of molecules and cells were about 3×10^7 and 5×10^6, respectively.

Continuum Approach

Most of the continuum computations were performed using a finite volume MUSCL total variation diminishing (TVD) scheme. The numerical fluxes on cell interfaces were computed by solving the Riemann problem with left and right states that are reconstructed from cell-averaged variables. It is well known that many conventional Riemann solvers are not reliable enough for computing flows that include strong shock waves and expansions. In such a case they may manifest many undesirable numerical phenomena, such as postshock oscillations and negative values of density and pressure. More robust solvers are usually characterized by a large numerical viscosity. Our strategy for overcoming this problem is to use a robust diffusive Riemann solver with a high-order MUSCL reconstruction. The HLLE solver[25] coupled with the fourth-order interpolation of Yamamoto and Daiguji[26] was used in this work. Such an approach allows one to capture the shock waves and to reduce the problems connected with smearing contact discontinuities and excessive numerical diffusion in smooth solution regions.

A body-fitted quadrilateral grid was used with the total number of nodes changed from 20,000 to 30,000 in different runs. To ensure the independence of the results on the grid resolution, some of the computations were repeated with finer grids (up to 50,000 nodes). The agreement between the coarse and fine grid results was very close.

To compute the flow around two symmetrical wedges with $\phi = 0$, the computational domain was divided into three zones, and a multiblock version of the Euler code was used.

The third-order explicit TVD Runge–Kutta scheme of Shu and Osher[27] was utilized for time stepping.

A uniform supersonic flow was specified at the inflow boundary, and nonreflecting conditions were taken at the upper and outflow boundaries. Nonpermeable conditions were imposed at the solid walls.

To examine the structure of a steady MR in more detail, several computations were performed in a rectangular domain cut from the channel. MR was obtained with a special statement of boundary conditions on the upper boundary. The flow parameters up to a certain point were taken from the Rankine–Hugoniot relations for an oblique shock with an appropriate incidence angle. After this point, the solid wall boundary conditions were taken. As a result, an expansion fan came from this point, and an incident shock wave emanated from the upper-left-hand corner of the domain. The computations for a rectangular box were conducted using a finite difference weighted essentially nonoscillatory (WENO) scheme of fifth order with global Lax–Friedrichs splitting.[28] The number of grid nodes in these computations was 96,000.

Two-Dimensional Shock Reflections

Hysteresis Effect

To investigate the hysteresis effect, the angle α was changed by wedge rotation around its trailing edge during the computations. This was achieved by the following procedure[5]: First the computation was performed for some α_0. After the flow became stationary, the wedge was rotated so that the new wedge position generated a shock wave with the incidence angle α_1 slightly different from α_0. When the flow became stationary in this position, the wedge was rotated again.

The computations start from $\alpha_0 < \alpha_N$, where RR is the only possible configuration. Then α is smoothly increased up to a value exceeding α_D using the aforementioned procedure. As both DSMC and continuum computations showed, the transition from RR to MR is observed between $\alpha_D = 39.2$ deg and $\alpha = 39.5$ deg. MR exists for $\alpha \geq 39.5$ deg. A typical example of the RR configuration, obtained in the dual-solution domain, is given in Fig. 3 (where N_x and N_y denote, respectively, the number of grid cells along x and y dimensions of the computational domain).

Note that using a coarse grid or large artificial viscosity in the continuum approach may cause retaining of RR up to the angles noticeably exceeding α_D (Ref. 13).

When α is smoothly decreased from $\alpha > \alpha_D$ using the same procedure, MR is observed in the dual-solution domain (Figs. 4 and 5). The transition from MR to RR occurs at α^*, which is slightly larger than α_N. For the continuum approach this is because for α approaching α_N the MS height becomes comparable with the cell size, and MR cannot be simulated any longer. In the kinetic approach this effect is caused by the influence of physical viscosity of the flow (see Ref. 5 for details). The exact values of α^* can be seen from Fig. 6, which shows the MS heights obtained in the Euler and DSMC simulations.

Thus, the computations clearly show the hysteresis effect when smoothly changing α from below and from above the dual-solution domain.

The results of kinetic and continuum computations are in good agreement for $Kn \sim 0.0005$. For larger Knudsen numbers the difference in α^* and H_{st} caused by viscous effects becomes visible; see Fig. 6. A decrease in the Knudsen number results in an increase in H_{st}, and the DSMC results tend to the inviscid solution. The latter agrees well with the experimental data[10] in almost the entire range of α variation. For $\alpha \gtrsim \alpha_D$ the Euler solution overpredicts the experimental data. This is explained by more profound three-dimensional effects in the experiments observed when increasing α.

Shape of MS

According to inviscid gasdynamics, the MS must be concave because the flow behind the MS near the triple point deflects

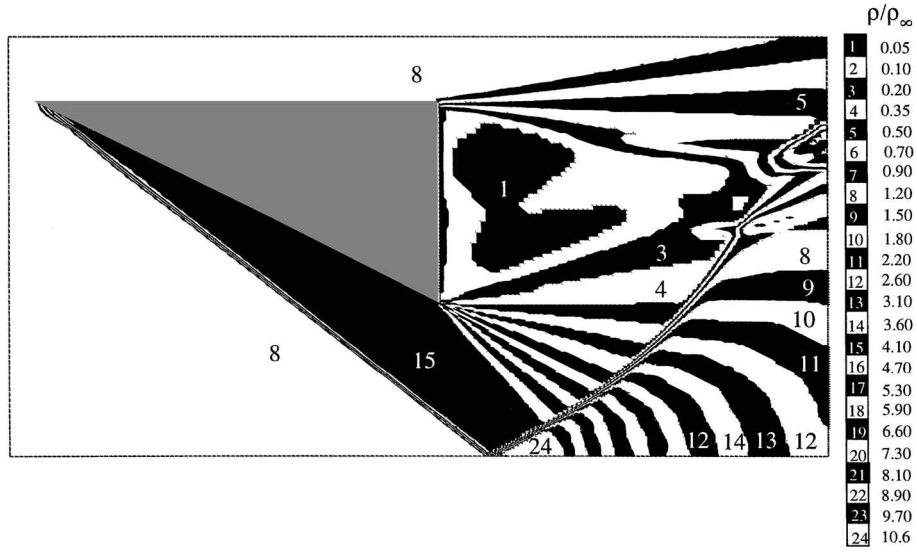

Fig. 3 Density field for RR at α = 38 deg; Euler solution; N_x = 175 and N_y = 130.

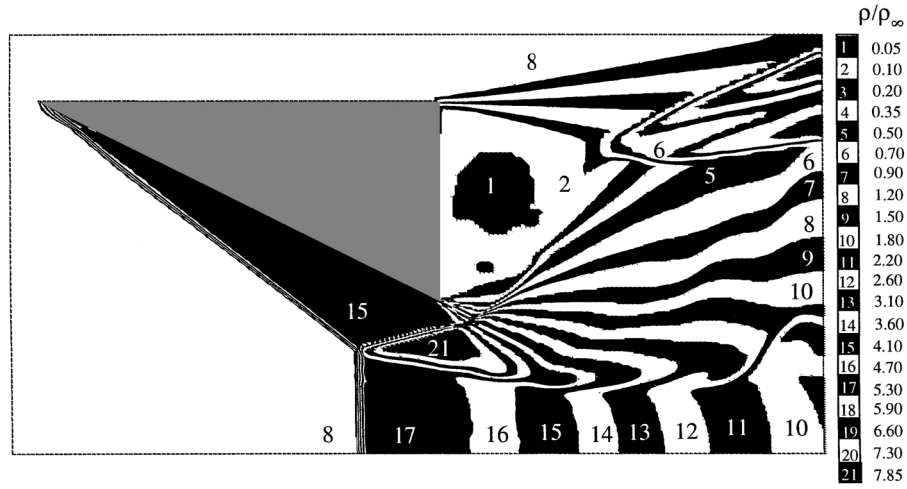

Fig. 4 Density field for MR at α = 38 deg; Euler solution; N_x = 175 and N_y = 130.

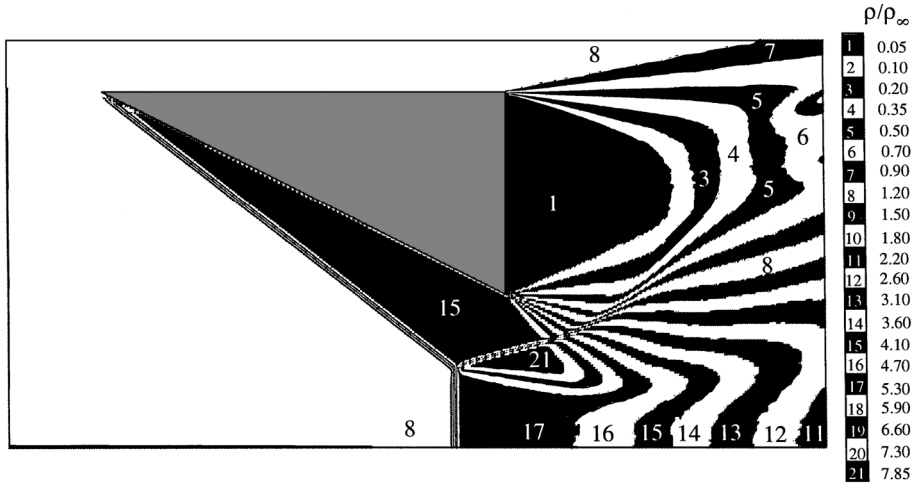

Fig. 5 Density field for MR at α = 38 deg; DSMC solution; Kn = 0.002.

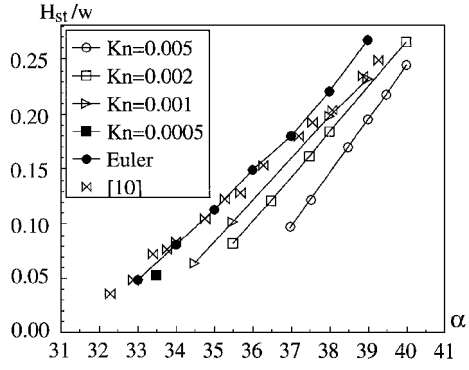

Fig. 6 Two-dimensional MS heights: computed and experimental[10] data.

toward the symmetry plane, whereas at the symmetry plane the flow does not deflect from its original direction. However, as has been noted in Ref. 29, the MS is commonly seen to be straight in the numerical simulations because its curvature is comparable with the grid step. To reveal the MS shape, we performed several computations with a higher space resolution. In these simulations, the rectangular computational domain cut from the channel was used.

The computations were performed using the continuum approach based on the solution of Euler equations. The density flowfield is given in Fig. 7a, where a theoretical three-shock solution is also presented. The angles of the incident and the reflected shock waves and the MS as well as the inclination of the slip surface near the reflection point coincide with the three-shock solution. A small curvature of the MS is distinctly visible.

In the mixing layer downstream of the triple point, vortices are observed that develop due to the Kelvin–Helmholtz instability. The vortices appear during the transient process, when the MS grows and moves upstream, and remain for a long time after the MS location stops changing. An emergence of new vortices is probably connected with a feedback mechanism, when the vortices produce an upstream influence through the subsonic region and cause an instability of the mixing layer near the triple point.

The Mach number flowfield is shown in Fig. 7b, which illustrates the flow acceleration in the virtual nozzle and the transformation from subsonic to supersonic flow in the throat. The sonic line is marked to demonstrate the shape of the subsonic region.

Influence of Initial Conditions

The existence of hysteresis upon smooth α variation shows that the choice of initial conditions is important for the final reflection configuration in the dual-solution domain. In this section, the influence of initial conditions is investigated for a constant angle of incidence (fixed wedges). The computations were performed for two different types of initial conditions and identical boundary conditions that specify a uniform freestream at the inflow boundary.

In the first computation, the initial condition was a uniform flow with the same parameters as at the inflow boundary. The density contours at different time moments during the flow evolution are

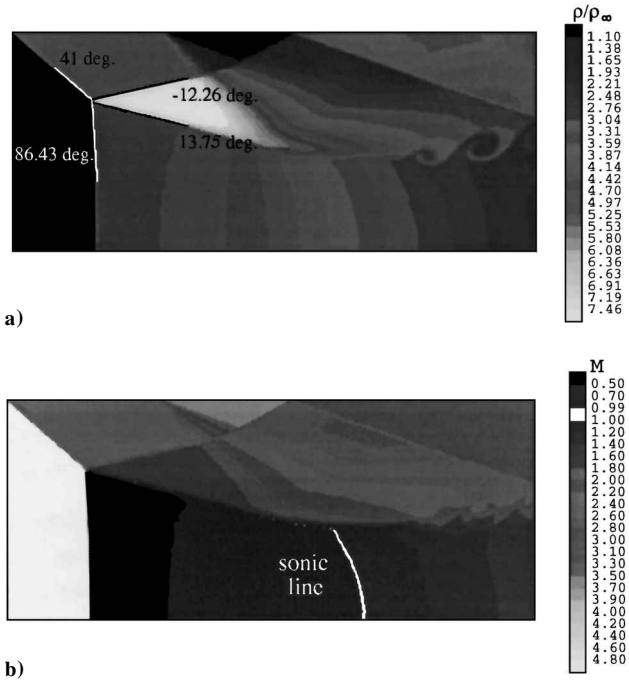

Fig. 7 a) Density and b) Mach number fields for MR simulation in rectangular domain at α = 41 deg; N_x = 480 and N_y = 200.

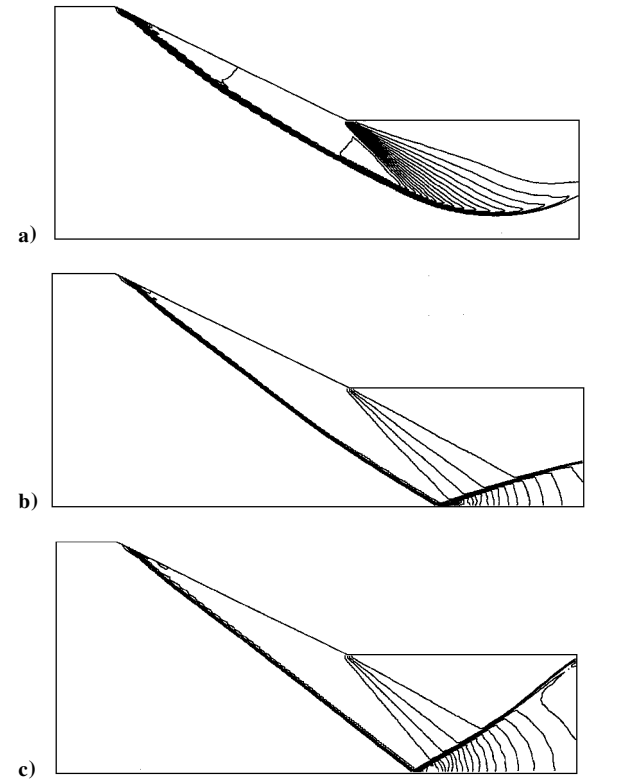

Fig. 8 Flow evolution with uniform flow as initial conditions; density field, α = 38 deg; Euler solution; N_x = 300 and N_y = 70.

given in Fig. 8 for $\alpha = 38$ deg. The wedge-generated shock wave is initially curved (Fig. 8a). It reaches the symmetry plane with a small angle of incidence, and RR is formed (Fig. 8b). This RR remains during subsequent evolution, and the final steady RR configuration is shown in Fig. 8c.

In the next computation, the gas in the computational domain is initially at rest and has the pressure p_i significantly smaller than the inflow value p_∞ ($p_i = 0.03p_\infty$). Therefore a gasdynamic discontinuity exists at the upstream boundary.

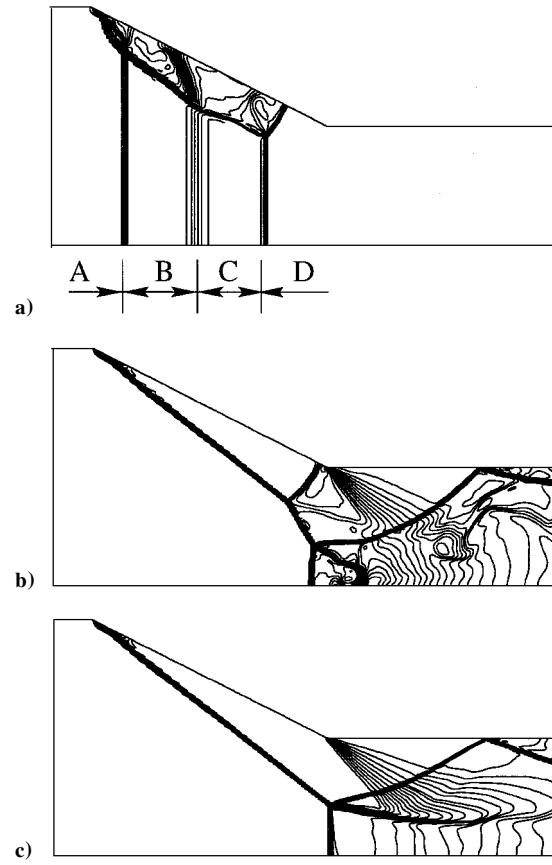

Fig. 9 Flow evolution with gas at rest as initial conditions; density field, α = 38 deg; Euler solution; N_x = 300 and N_y = 70.

The flow evolution for these initial data is shown in Fig. 9. Two shock waves are formed, separated by the contact discontinuity. Four different regions can be identified (Fig. 9a): region D of the gas at rest, region C between the first shock and the contact discontinuity where the Mach number cannot exceed the maximum $M = \sqrt{[2/\gamma(\gamma - 1)]}$ (1.89 for $\gamma = 1.4$), region B between the contact discontinuity and the second shock wave, and region A of the freestream flow. The Mach number in region B is also smaller than M_∞, and the slope of the wedge-generated shock wave in region B is larger than that for the incident shock wave in region A. Figure 9b demonstrates a sharp bend of the incident shock wave on the boundary between regions A and B. The MS develops from the large-angle shock incident to the symmetry plane in region B. Finally, MR forms as a stationary configuration (Fig. 9c).

More detailed computations for the second type of initial conditions showed that the final configuration depends on the value of p_i. Namely, for all values $p_i < p^*$ RR is realized, whereas for $p^* < p_i < p^{**}$ MR is developed, and for $p_i > p^{**}$ the choked shock wave is the final configuration. This conclusion is valid for both numerical approaches. The values of p^* and p^{**} are slightly different for these approaches and depend on the distance between the inflow boundary and the wedge leading edge and on the Knudsen number used in DSMC computations.

Freestream Perturbations

As both RR and MR were observed in the numerical calculations inside the dual-solution domain, these configurations are stable to infinitesimal perturbations. However, large-amplitude perturbations may cause a flip between two configurations. Any experimental facility has a certain level of perturbations that differ in their nature and magnitude. The aim of numerical simulations is to model the perturbations of a specific type and to analyze their influence on the hysteresis phenomena.

Vuillon et al.[30] investigated the stability of regular reflection by introducing perturbations behind the reflection point. (They set the velocity to zero in the several rows of grid cells.) Here we consider

the influence of strong but short-time perturbations of the freestream that seem to be more physical (see also Refs. 6 and 31). The computations showed that such perturbations may transform RR to MR and back. The Euler results on the impact of an impulsive perturbation on RR are given in Fig. 10 for $\alpha = 34.5$ deg. The perturbation consisted of the increase in the freestream velocity at the upstream boundary by 40%. It was applied during a short time, $\tau = H_{st}/U_\infty$, where H_{st} is the MS height for the corresponding MR and U_∞ is the freestream velocity. After the perturbations had interacted with the RR configuration, MR was formed. Obviously, the reason for the MR formation is a temporary existence of the shock wave with a large angle of incidence during this unsteady interaction.

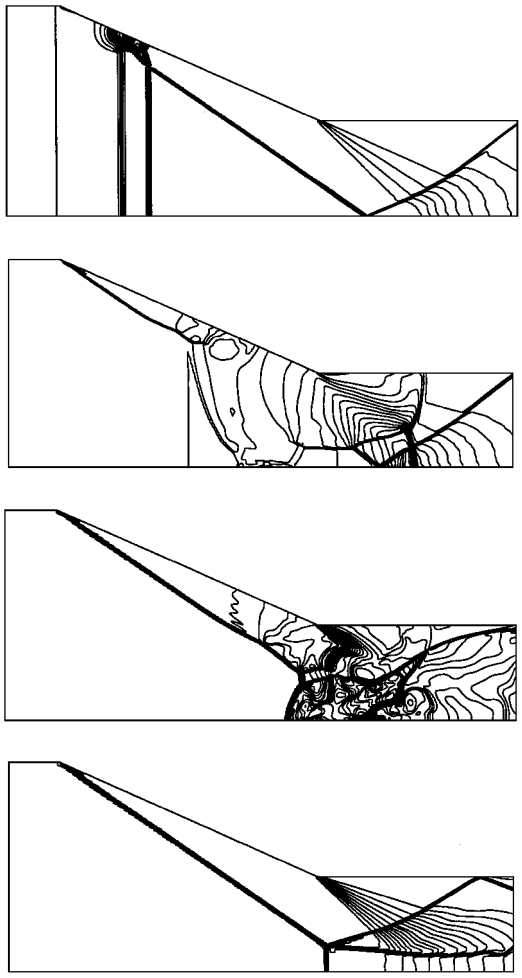

Fig. 10 Flow evolution during RR to MR transition by flow perturbation; density field, α = 34.5 deg; Euler solution; N_x = 240 and N_y = 120.

The reverse transition from MR to RR by means of impulsive freestream perturbations (the freestream velocity was decreased for a short time) was also observed in computations (see also Ref. 9). The computations performed show that the transition from RR to MR in the greater part of the dual-solution domain is easier to cause than the reverse transition, where stronger perturbations have to be applied. Note that the MS height does not depend on the way of obtaining the Mach configuration and is defined only by the flow geometry.

Three-Dimensional Computations

The flow three-dimensionality may considerably affect the transition process and is one of the possible reasons for the inconsistency between experimental data and two-dimensional numerical results.[10,32,33] It is next to impossible to preserve the two-dimensionality of the flow in experiment. When $\alpha \to \alpha_D$, the Mach number behind the reflected shock wave of RR is about unity, and the influence of side effects may extend inward up to the vertical symmetry plane. For MR, the existence of a subsonic region behind the MS even increases the requirements to the aspect ratio.

Both von Neumann and detachment criteria were obtained for the two-dimensional case. For three-dimensional flow, the analytical treatment is more complicated and has not been done yet. An application of two-dimensional criteria to three-dimensional flow is questionable and requires a substantiation for each particular case.

The main objective of the computations is to clarify the influence of the aspect ratio on the transition angles and final shock configuration.

Both kinetic and continuum approaches have shown that significant three-dimensionality delays the transition from RR to MR. For $z/w = 1$, a regular configuration retains even at $\alpha = 40$ deg $> \alpha_D$ (Fig. 11). Note that the bending of the incident shock wave in the spanwise direction results in the formation of a MS surface on the periphery. (See the plane normal to the freestream.) This is because the three-dimensional reflected shock wave there can no longer turn the flow parallel to the horizontal symmetry plane. The flow behind the peripheral MS surface is supersonic. The MR configuration in the core flow is observed only at $\alpha = 42$ deg. The Mach number contours for this case are given in Fig. 12. The size of the subsonic zone in the transversal direction is about the wedge spanwise size z.

When increasing the aspect ratio, the angle of RR to MR transition approaches α_D. For example, for $z/w = 2.14$ the MR was observed at $\alpha = 40$ deg (Fig. 13). The process of MR formation is as follows: Initially, a small MS is formed near the vertical symmetry plane, and RR remains between this MS and the peripheral MS surface. Then, if the aspect ratio is large enough, the core flow MS develops upstream and outward and merges with the peripheral MS (for details see Ref. 9).

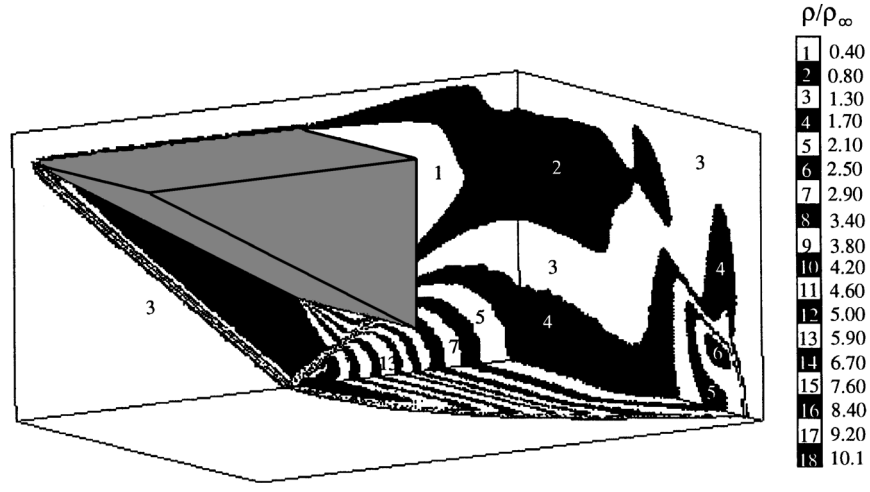

Fig. 11 Three-dimensional regular reflection at α = 40 deg, z/w = 1; density field; DSMC solution; Kn = 0.005.

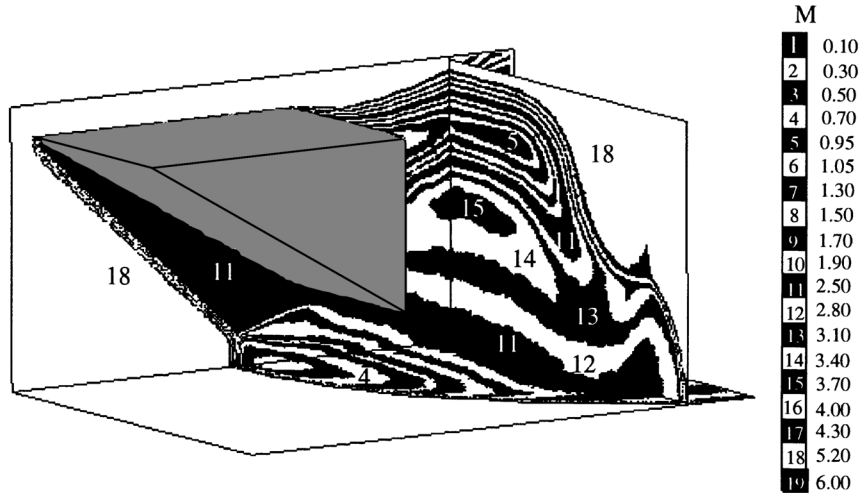

Fig. 12 Three-dimensional MR at α = 42 deg, z/w = 1; Mach number field; DSMC solution; Kn = 0.005.

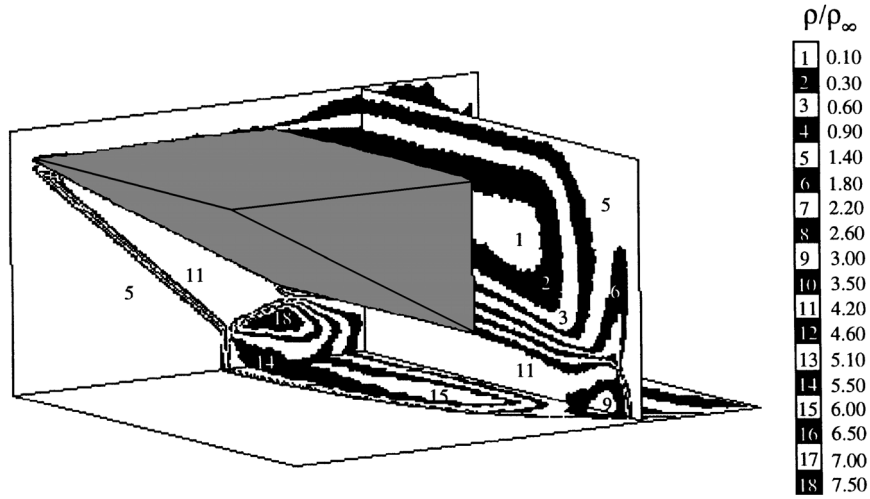

Fig. 13 Three-dimensional MR at α = 40 deg, z/w = 2.14; density field; DSMC solution; Kn = 0.005.

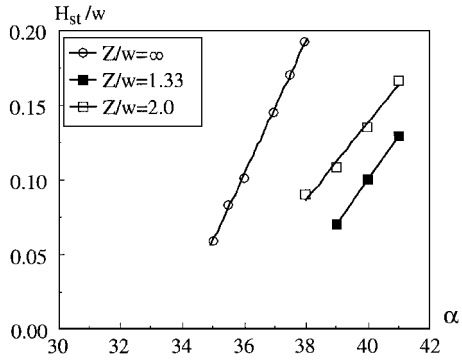

Fig. 14 MS heights for different aspect ratios.

The hysteresis effect has also been observed in three-dimensional computations. However, two-dimensional transition criteria cannot be applied for this case; the angles of both forward and reverse transitions depend on the aspect ratio and increase when z/w decreases.

The aspect ratio affects not only the transition angles but also the MS height. The influence of the aspect ratio on the MS is given in Fig. 14 for two-dimensional ($z/w = \infty$) and three-dimensional ($z/w = 1.33$ and 2) cases.

These computations were performed for $H/w = 0.75$ (parameters corresponding to the experimental conditions[4]). For such a geometry, it is impossible to obtain MR in two-dimensional flow for $\alpha > 38$ deg because the reflected shock wave comes to the wedge surface, and a choked shock configuration develops. The existence of MR for angles up to 45 deg observed in the experiment[4] gives evidence of a considerable flow three-dimensionality.

As seen in Fig. 14, if the aspect ratio increases, the MS height in three-dimensional flow tends to the two-dimensional value. Nevertheless, this tendency is very gradual, and even assuming linear dependence of the MS height on the aspect ratio, the two-dimensional case will be reached only at $z/w > 4$. This result has to be taken into account when elaborating a strategy for further experimental works.

Conclusions

Comprehensive numerical investigations of the transition between regular and MR and attendant hysteresis phenomenon in two-dimensional and three-dimensional steady flows have been performed by the kinetic (the DSMC method) and continuum (the solution of Euler equations) approaches.

A detailed examination of the MS configuration has shown that the MS is slightly concave. This is in accordance with the inviscid gasdynamics theory.

An analysis of the formation of shock wave configurations has been conducted for two types of initial conditions. The first type was a uniform flow, and RR is the final configuration everywhere inside the dual-solution domain. In the second case the computational domain was initially filled with gas at rest. In this case, either RR, MR, or a choked shock wave can be formed, depending on the pressure of gas at rest.

The effect of impulsive freestream perturbations on the shock configuration in the dual-solution domain has been studied. These perturbations may cause a flip from RR to MR and back. MR is

more stable to perturbations, and the transformation of RR to MR is easier to obtain than the reverse one.

The computations also reveal the hysteresis effect in three-dimensional computations. As the investigation of the aspect ratio effect shows, the flow three-dimensionality increases the angles of both forward and reverse transitions and decreases in the MS height.

Acknowledgments

This research was supported by INTAS under Grant 96-2356 and the Russian Foundation for Basic Research under Grant 98-01-00677.

References

[1]Hornung, H. G., Oertel, H., and Sandeman, R. J., "Transition to Mach Reflection of Shock Waves in Steady and Pseudosteady Flow with and Without Relaxation," *Journal of Fluid Mechanics*, Vol. 90, 1979, pp. 541–560.

[2]Hornung, H. G., and Robinson, M. L., "Transition from Regular to Mach Reflection of Shock Waves, Part 2. The Steady Flow Criterion," *Journal of Fluid Mechanics*, Vol. 123, 1982, pp. 155–164.

[3]Chpoun, A., Passerel, D., Lengrand, J.-C., Li, H., and Ben-Dor, G., "Mise en Évidence expérimentale et numérique d'un Phénomène d'Hystérésis lors de la Transition Réflexion de Mach—Réflexion Régulière," *Academie de Science Paris: Comptes Rendus*, T.319, Série 2, 1994, pp. 1447–1453.

[4]Chpoun, A., Passerel, D., Li, H., and Ben-Dor, G., "Reconsideration of Oblique Shock Wave Reflections in Steady Flows, Part 1. Experimental Investigation," *Journal of Fluid Mechanics*, Vol. 301, 1995, pp. 19–35.

[5]Ivanov, M. S., Gimelshein, S. F., and Beylich, A. E., "Hysteresis Effect in Stationary Reflection of Shock Waves," *Physics of Fluids*, Vol. 7, No. 4, 1995, pp. 685–687.

[6]Ivanov, M. S., Beylich, A. E., Gimelshein, S. F., and Markelov, G. N., "Numerical Investigation of Shock Wave Reflection Problems in Steady Flows," *Proceedings of the 20th International Symposium on Shock Waves* (Pasadena, CA), World Scientific, Singapore, 1995, pp. 471–476.

[7]Ivanov, M. S., Zeitoun, D., Vuillon, J., Gimelshein, S. F., and Markelov, G. N., "Investigation of the Hysteresis Phenomena in Steady Shock Reflection Using Kinetic and Continuum Methods," *Shock Waves*, Vol. 5, No. 6, 1996, pp. 341–346.

[8]Ivanov, M. S., Gimelshein, S. F., Kudryavtsev, A. N., and Markelov, G. N., "Numerical Study of the Transition from Regular to Mach Reflection in Steady Supersonic Flows," *Proceedings of 15th International Conference on Numerical Methods in Fluid Dynamics* (Monterey, CA), Vol. 490, Lecture Notes in Physics, Springer–Verlag, Berlin, 1997, pp. 394–399.

[9]Ivanov, M. S., Kudryavtsev, A. N., Markelov, G. N., and Gimelshein, S. F., "Transition Between Regular and Mach Reflection of Shock Waves in Steady Flows," AIAA Paper 97-2511, June 1997.

[10]Ivanov, M. S., Klemenkov, G. P., Kudryavtsev, A. N., Nikiforov, S. B., Pavlov, A. A., Fomin, A. A., Kharitonov, A. M., Khotyanovsky, D. V., and Hornung, H. G., "Experimental and Numerical Study of the Transition Between Regular and Mach Reflections of Shock Waves in Steady Flows," *Proceedings of 21st International Shock Waves Symposium* (Great Keppel Island, Australia), Panther, Fyshwick, Australia, 1997, pp. 819–824.

[11]von Neumann, J., "Oblique Reflection of Shocks," U.S. Dept. of Commerce Office of Tech. Serv., PB-37079, Washington, DC, 1943; see also *Collected Works*, edited by A. H. Taub, Vol. 6, Pergamon, Oxford, England, UK, 1963, pp. 238–299.

[12]Vuillon, J., Zeitoun, D., and Ben-Dor, G., "Numerical Investigations of the Prediction of the Mach-Stem Height in Steady Flows," *Proceedings of the 20th International Symposium on Shock Waves* (Pasadena, CA), Vol. 1, World Scientific, Singapore, 1995, pp. 459–464.

[13]Chpoun, A., and Ben-Dor, G., "Numerical Confirmation of the Hysteresis Phenomenon in the Regular to the Mach Reflection Transition in Steady Flows," *Shock Waves*, Vol. 5, No. 4, 1995, pp. 199–203.

[14]Ivanov, M. S., Kashkovsky, A. V., Gimelshein, S. F., and Markelov, G. N., "Statistical Simulation of Hypersonic Flows from Free-Molecular to Near-Continuum Regimes," *Thermophysics and Aeromechanics*, Vol. 4, No. 3, 1997, pp. 251–268.

[15]Shirozu, T., and Nishida, M., "Numerical Studies of Oblique Shock Wave Reflection in Steady Two-Dimensional Flows," *Memoirs of the Faculty of Engineering, Kyushu University*, Vol. 55, No. 2, 1995, pp. 193–204.

[16]Schotz, M., Levy, A., Ben-Dor, G., and Igra, O., "Analytical Prediction of the Wave Configuration Size in Steady Mach Reflections," *Shock Waves*, Vol. 7, No. 6, 1997, pp. 363–372.

[17]Li, H., and Ben-Dor, G., "A Parametric Study of Mach Reflection in Steady Flows," *Journal of Fluid Mechanics*, Vol. 341, 1997, pp. 101–125.

[18]Ben-Dor, G., Elperin, T., Li, H., Vasiliev, E., and Chpoun, A., "Dependence of Steady Mach Reflections on the Reflecting-Wedge Trailing-Edge Angle," *AIAA Journal*, Vol. 35, No. 11, 1997, pp. 1780–1782.

[19]Leclerc, E., Lengrand, J. C., and Chpoun, A., "Experimental Investigation of the Influence of Downstream Flow Conditions on Mach Stem Height," *Proceedings of 21st International Symposium on Shock Waves* (Great Keppel Island, Australia), Panther, Fyshwick, Australia, 1997, pp. 853–856.

[20]Chow, W. L., and Chang, I. S., "Mach Reflection from Overexpanded Nozzle Flow," *AIAA Journal*, Vol. 10, No. 9, 1972, pp. 1261–1263.

[21]Chow, W. L., and Chang, I. S., "Mach Reflection Associated with Over-Expanded Nozzle Free Jet Flows," *AIAA Journal*, Vol. 13, No. 6, 1975, pp. 762–766.

[22]Li, H., and Ben-Dor, G., "Mach Reflection Wave Configuration in Two-Dimensional Supersonic Jets of Overexpanded Nozzles," *AIAA Journal*, Vol. 36, No. 3, 1998, pp. 488–491.

[23]Ivanov, M. S., and Rogasinsky, S. V., "Theoretical Analysis of Traditional and Modern Schemes of the DSMC Method," *Proceedings of the XVIIth International Symposium on Rarefied Gas Dynamics* (Aachen, Germany), VCH, Weinheim, Germany, 1990, pp. 629–642.

[24]Borgnakke, C., and Larsen, P. S., "Statistical Collision Model for Monte Carlo Simulation of Polyatomic Gas Mixture," *Journal of Computational Physics*, Vol. 18, No. 3, 1975, pp. 405–420.

[25]Einfeldt, B., Munz, C. D., Roe, P. L., and Sjögren, B., "On Godunov-Type Methods near Low Densities," *Journal of Computational Physics*, Vol. 92, No. 2, 1991, pp. 273–295.

[26]Yamamoto, S., and Daiguji, H., "Higher-Order-Accurate Upwind Schemes for Solving the Compressible Euler and Navier–Stokes Equations," *Computers and Fluids*, Vol. 22, No. 2/3, 1993, pp. 259–270.

[27]Shu, C.-W., and Osher, S., "Efficient Implementation of Essentially Non-Oscillatory Shock-Capturing Schemes," *Journal of Computational Physics*, Vol. 77, No. 2, 1988, pp. 439–471.

[28]Jiang, G.-S., and Shu, C.-W., "Efficient Implementation of Weighted ENO Schemes," *Journal of Computational Physics*, Vol. 126, No. 1, 1996, pp. 202–228.

[29]Vuillon, J., Zeitoun, D., and Ben-Dor, G., "Numerical Investigation of Shock Wave Reflections in Steady Flows," *AIAA Journal*, Vol. 34, No. 6, 1996, pp. 1167–1173.

[30]Vuillon, J., Zeitoun D., and Ben-Dor, G., "Reconsideration of Oblique Shock Wave Reflections in Steady Flows. Part 2. Numerical Investigation," *Journal of Fluid Mechanics*, Vol. 301, 1995, pp. 37–50.

[31]Ivanov, M. S., Gimelshein, S. F., and Markelov, G. N., "Statistical Simulation of the Transition Between Regular and Mach Reflection in Steady Flows," *Computers and Mathematics with Applications*, Vol. 35, No. 1/2, 1998, pp. 113–125.

[32]Fomin, V. M., Ivanov, M. S., Kharitonov, A. M., Klemenkov, G. P., Kudryavtsev, A. N., Pavlov, A. A., and Hornung, H. G., "The Study of Transition Between Regular and Mach Reflection of Shock Waves in Different Wind Tunnels," *Proceedings of 12th International Mach Reflection Symposium* (Pilanesberg, South Africa), Univ. of the Witwatersrand, Johannesburg, Republic of South Africa, 1996, pp. 137–151.

[33]Skews, B. W., "Aspect Ratio in Wind Tunnel Studies of Shock Wave Reflection Transition," *Shock Waves*, Vol. 7, No. 6, 1997, pp. 373–383.

K. Kailasanath
Associate Editor